Algebraic and the graphic depictions of stabilized multipartite unlockable bound entanglement

Li-Yi Hsu and Keng-Shuo Wu
Department of Physics, Chung Yuan Christian University, Chungli 32023, Taiwan, Republic of China
(Received 21 June 2009; published 23 October 2009)

In this paper, we investigate multipartite unlockable stabilized bound entanglement. First, the mathematical structure of these stabilized bound entangled states is studied. Second, since stabilizer states are the local equivalent to the graph states, we study such stabilized mixed states in the graph-state formalism. As a result, the unlockable stabilized bound entangled states can be graphically depicted and decomposed in the product form. Some examples are discussed.

DOI: 10.1103/PhysRevA.80.042324 PACS number(s): 03.67.Mn

I. INTRODUCTION

Entanglement is the most peculiar phenomenon in quantum physics. In quantum information processing, entanglement now has been regarded as a physical resource. For example, the two-qubit Bell states can be exploited in one-qubit teleportation [1], dense coding of two classical bits [2], quantum key distribution [3], and other applications. In physical realization, environments always spoil the pure entangled states into mixed ones. As a result, entanglement distillation against such random disturbance is an essential challenge in quantum information technology. By definition, a mixed entangled state is said to be distillable if pure entanglement can be obtained using local operations and classical communication (LOCC) [4]. On the other hand, however, there exist mixed entangled states, which are also known as bound entanglement states (BESs), which do not allow for entanglement distillation [5]. Although BESs can be undistillable, some of them can be stabilized. Smolin initially introduced a four-qubit BES, known as Smolin state, which can be stabilized [6]. Recently, stabilized bound entangled states (SBESs) have been demonstrated to be useful for quantum information processing. For example, SBESs can be exploited in reducing communication complexity [7], remote quantum information concentration [8,9], quantum secret sharing, and nonadditivity of quantum channels with multiple receivers [10]. Also, the nonlocality of certain SBESs can be demonstrated via the violation of Bell-type inequalities [7].

In this paper, we focus on unlockable SBESs (USBESs). The SBESs are unlockable or activated in the following sense. The pure entanglement can be distillable when the qubits are divided into several groups. Therein, the collective quantum operations on qubits in the same group can be performed. For example, Bandyopadhyay *et al.* considered the generalized 2N-qubit Smolin BESs, and demonstrated that these states are can be unlocked and superactivated [11]. Very recently, the stabilizer formalism of USBESs has been proposed by Wang and Ying [12].

On the other hand, under local Clifford operations, any (inseparable) stabilizer state is local equivalent to a (connected) graph state. Therefore, the segments of stabilizer generators in any partition are local equivalent to the stabilizer generators of a connected stabilizer state. From this perspective, we propose how to construct USBESs in the graph-state formalism. Graph states are "visible," since there is always an associated graph for any given graph state. As a result, it will be shown that the USBESs can also become visible. Under the proposed approach, another advantage is that the above conditions for USBESs are automatically satisfied.

The paper is organized as follows. In Sec. II, we present some simple but essential mathematics exploited in constructing the USBESs. In Sec. III, we study the USBES in the graph-state formalism. Wherein, the corresponding density matrix can be graphically decomposed. Some discussions are made in Sec. IV.

II. MATHEMATICS OF UNLOCKABLE STABILIZED BOUND ENTANGLED STATES

Before proceeding further, according to the Theorem 1 of Ref. [12], we briefly review the formal definition of an USBES, S, as follows. Suppose $g_1, g_2, \ldots, g_3$ are commuting elements that stabilize S. If

Condition 1. S is separable with respect to some specific partition $\{Q_1, Q_2, \ldots, Q_M\}$;

Condition 2. there exists a partition $\{T_1, T_2, \ldots, T_k\}$ with $|T_1| > 1$ such that S is separable with respect to this partition and $g_1^{T_1}, g_2^{T_1}, \ldots, g_k^{T_1}$ form a complete set of stabilizer generators on T_1. Then the maximally mixed state S is an USBES.

For more details, readers can refer to Ref. [12]. The construction of N-qubit USBESs is essentially based on the following simple algebraic equations. Denote two binary vectors $\vec{x} = (x_1, \ldots, x_m)$ and $\vec{\gamma} = (\gamma_1, \ldots, \gamma_m)$, where each x_i and $\gamma_i \in \{0,1\} \forall \; i \in \{1, \ldots, m\}$. Here, $\vec{x}$ and $\vec{\gamma}$ are dual to each other. That is

$$\vec{x} \cdot \vec{\gamma} = 0 \bmod 2. \tag{1}$$

In the following, $\vec{x}$ is a nonzero vector. For a given $\vec{x}$, all legitimate vectors $\vec{\gamma}$s can be regarded as codewords and form a $(m-1)$-dimensional closed linear subspace C. Here, the codespace C can be spanned by $(m-1)$ vectors $e_1, \ldots, e_{m-1}$ and a legitimate $\vec{\gamma}$ can be expressed as

$$\vec{\gamma} = \sum_{i=0}^{m-1} \alpha_i e_i,$$

where each $\alpha_i \in \{0,1\}$. On the other hand, $\vec{x}$ and zero vectors $\vec{0}$ form the closed linear subspace $C^{\perp}$, which is the dual of C.

In general, for a given classical linear code, there exists a parity check matrix, H, such that

$$He_i = 0.$$

Equivalently, $\vec{x}$ can be regarded as $1 \times m$ parity check matrix. A useful formula is [13]

$$\sum_{\vec{\gamma} \in C} (-1)^{\vec{u} \cdot \vec{\gamma}} = \begin{cases} 2^{m-1} & u \in C^{\perp} \\ 0 & u \notin C^{\perp} \end{cases} . \tag{2}$$

With Eq. (1) as the constraint, we have

$$\sum_{\vec{\gamma} \in C} \prod_{i=1}^{m} \left(\frac{\mathbf{1} + (-1)^{\gamma_i} g_i}{2} \right) = \frac{\mathbf{1} + \Pi_{i=1}^{m} g_i^{x_i}}{2}, \tag{3}$$

where $\mathbf{1}$ denotes the identity operator and $\{g_1, \ldots, g_m\}$ is a set of commuting operators.

Proof of Eq. (3). Note that, the left-hand side of Eq. (3), can be expanded as

$$\frac{1}{2^m} \sum_{i=1}^{m} \sum_{\vec{\gamma} \in C} (-1)^{\vec{y} \cdot \vec{\gamma}} g_i^{y_i},$$

where $\vec{y} = (y_1, \ldots, y_m)$ and each $y_i \in \{0,1\}$. According to Eq. (2), the sum are nonvanishing only when $\vec{y} \in \{\vec{x}, \vec{0}\}$. This completes the proof. ■

Equation (3) can be extended as follows. Without loss of generality, $1 < n_1 \leq n_2 \leq \ldots \leq n_m$ is assumed. Denote the given n_m binary vector $\vec{x_j} = (x_{1_j}, \ldots, x_{m_j})$, $1 \leq j \leq n_m$, as the $1 \times m$ parity matrix, H, of the $(m-1)$ classical linear code with the codespace, C_j, with a legitimate codeword vector $\vec{\gamma_j} = (\gamma_{1_j}, \ldots, \gamma_{m_j})$. We have

$$\vec{x_j} \cdot \vec{\gamma_j} = 0 \bmod 2, \tag{4}$$

and hence

$$\sum_{all\ \Gamma_G} \prod_{i=1}^{m} \left\{ \prod_{j=1}^{n_i} \left(\frac{\mathbf{1} + (-1)^{\gamma_{i_j}} g_{i_j}}{2} \right) \right\} = \prod_{j=1}^{n_m} \left(\frac{\mathbf{1} + \overline{g_j}^{\vec{x}_j}}{2} \right), \tag{5}$$

where the vector set $\Gamma_G = \{\vec{\gamma_1}, \ldots, \vec{\gamma_m}\}$, and

$$\overline{g_j}^{\vec{x}_j} = \prod_{i=1}^{m} g_{i_j}^{x_{i_j}}.$$

Notably, the set $S = \{g_{1_1}, \ldots, g_{m_{(n_m)}}\}$ is a set of commuting operators. In the following, each element in S is the multiplication by either the identity matrix or the Pauli matrices:

$$X = \begin{pmatrix} 0 & 1 \\ 1 & 0 \end{pmatrix}, \quad Y = \begin{pmatrix} 0 & -i \\ i & 0 \end{pmatrix}, \quad Z = \begin{pmatrix} 1 & 0 \\ 0 & -1 \end{pmatrix},$$

acting on each qubits. We denote X_j the matrix X acting on the j-th qubit, and similarly for Y_j and Z_j. Some remarks are made as follows. First, the right-hand side of Eq. (5) can be recognized as the density matrix of the N-qubit USBES. Wherein, the normalization constant $2^{-\Sigma_{i=1}^{m} n_i}$ is ignored. These n_m operators $\overline{g_j}^{\vec{x}_j}$, where $j = 1, \ldots, n_m$, can be regarded as the stabilizer generators of the USBES. Second, in the left-hand side of Eq. (5),

$$\prod_{j=1}^{n_i} \left(\frac{\mathbf{1} + (-1)^{\gamma_{i_j}} g_{i_j}}{2} \right) \tag{6}$$

can be recognized as the density matrix of the pure state which is the common eigenstate of the commuting and independent operators g_{i_1}, …, and $g_{i_{(n_i)}}$ with eigenvalues $(-1)^{i_1}$, …, and $(-1)^{i_{(n_i)}}$, respectively. There are n_i qubits that comprise the pure state in Eq. (6). As a result,

$$N = \sum_{i=1}^{m} n_i, \tag{7}$$

In the following it is further required that the pure state with the corresponding density in Eq. (6) is an entangled state.

To verify that Eq. (5) is a density matrix of an USBES, define the Q_i= [the n_i qubits comprising the density matrix of the pure state in Eq. (6)]. To satisfy condition 1, it is obviously to verify that, according to Eqs. (5) and (6), arbitrary two qubits belonging different partitions, Q_i and Q_j, must be separable. To satisfy condition 2, without loss of generality, it is required that $x_{i_j} = 1$ for $\forall\ j \in \{1, \ldots, n_i\}$. In this case, $T_1 = Q_i$, the segments of the stabilizer generators $\overline{g_j}^{\vec{x}_j}$ of the USBES in T_1 are g_{i_j}. Since the state of Eq. (6) is entangled, the Abelian subgroup $\langle g_{i_1}, \ldots, g_{i_{n_i}} \rangle$ is inseparable and forms a complete set of stabilizer generators. As a result, not any given vector set $X = \{\vec{x_1}, \ldots, \vec{x_m}\}$ can always be exploited to construct an USBES. For example, if $x_{i_j} = \delta_{ij}$, the Eq. (5) cannot be a density matrix of an USBES. Another constraint is that, for $\forall\ i = 1, \ldots, m$, a legitimate set X for an USBES must the make $\gamma_{i_1}, \ldots, \gamma_{i_{(n_i)}}$ random distributed and hence

$$\sum_{\gamma_{i_1}, \cdots, \gamma_{i_{(n_i)}}} \prod_{j=1}^{n_i} \left(\frac{\mathbf{1} + (-1)^{\gamma_{i_j}} g_{i_j}}{2} \right) \sim \mathbf{1}. \tag{8}$$

In other words, the n_i-qubit state in Eq. (8) is maximally mixed. As an example, if $x_{i_j} = 1 \forall\ i, j$, it is easy to verify that all $\gamma_{i_j} s$ each must be random distributed (see Sec. III).

Finally, it is noteworthy that the set of commuting operators, S, is not unique. It is not surprising from the perspective of physical realization. There are infinite ways of preparing a mixed state. As an illustration, in example 1, it will be shown that, the four-qubit mixed state with right-hand side of Eq. (5) as density matrix can be prepared in different ways.

Example 1. Consider the four-qubit bound state ($n=4$), where the density matrix is

$$\rho_2 = \frac{1}{4} \left(\frac{\mathbf{1} + X_1 Z_2 X_3 Z_4}{2} \right) \left(\frac{\mathbf{1} + Z_1 X_2 Z_3 X_4}{2} \right). \tag{9}$$

It is noteworthy that ρ_2 local equivalent to the density matrix of four-qubit Smolin state [6]. To derive ρ_2, the parameters in Eqs. (4) and (5) are set as follows: $m = n_1 = n_2 = 2$ and $x_{1_1} = x_{2_1} = x_{2_1} = x_{2_2} = 1$. As a result, two constraints are

$$\gamma_{1_1} + \gamma_{2_1} = 0 \tag{10}$$

and

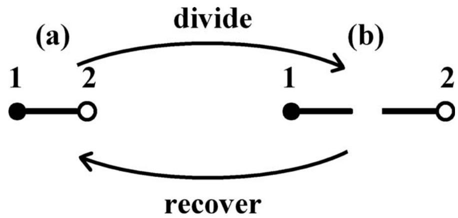

FIG. 1. The dividing and recovering of an edge. Two divided edges can be recovered into the connected two-vertex colored graph, where the associated graph state is $Z_1|\mathrm{G}_2\rangle$. Notably, there is no unconnected end after the recovery.

$$\gamma_{1_2}+\gamma_{2_2}=0, \tag{11}$$

respectively. In addition, let either

$$g_{1_1}=X_1Z_2, \quad g_{1_2}=Z_1X_2, \quad g_{2_1}=X_3Z_4, \quad \text{and} \quad g_{2_2}=Z_3X_4. \tag{12}$$

or

$$g_{1_1}=X_1Z_4, \quad g_{1_2}=Z_1X_4, \quad g_{2_1}=X_3Z_2, \quad \text{and} \quad g_{2_2}=Z_3X_2. \tag{13}$$

It will be seen the stabilizer generators in Eqs. (12) and (13) are those of the two-qubit graph states. Alternatively, the commuting operators can be also set as

$$g_{1_1}=X_1X_3, \quad g_{1_2}=Z_1Z_3, \quad g_{2_1}=Z_2Z_4, \quad \text{and} \quad g_{2_2}=X_2X_4. \tag{14}$$

III. GRAPHIC DECOMPOSITION OF UNLOCKABLE STABILIZED BOUND ENTANGLED STATES

A. Review of graph states

In this section, we will focus on the visualization of the USBESs. Before proceeding further, we briefly review the graph states as follows. We denote a given n-qubit graph state by $|\mathrm{G}_n\rangle$. The associated graph of $\mathrm{G}_n=(\mathrm{V},\mathrm{E})$ can be composed of a set V of n vertices and a set E of edges. The neighboring set of the vertex i is denoted by $\mathrm{N}(i)=\{j|(i,j)\in \mathrm{E}\}$. Notably, for the vertex i, there correspond the stabilizer generators, g_i

$$\mathrm{g}_i=X_i\prod_{j\in N(i)}Z_j, \ \forall \quad i=1,\ldots,n, \tag{15}$$

and $|\mathrm{G}_n\rangle$ is stabilized by g_i. In addition, it is obvious that

$$\{Z_i,g_i\}=0, \tag{16}$$

where {,} is the anticommutator. In the following, we define the generalized n-qubit *colored* graph state as $\Pi_{j=1}^{n}Z_j^{\gamma_j}|\mathrm{G}_n\rangle$. According to Eqs. (15) and (16), the corresponding density matrix is

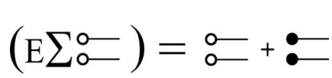

FIG. 2. Two-vertex case of all colored graph configurations with even filled vertices.

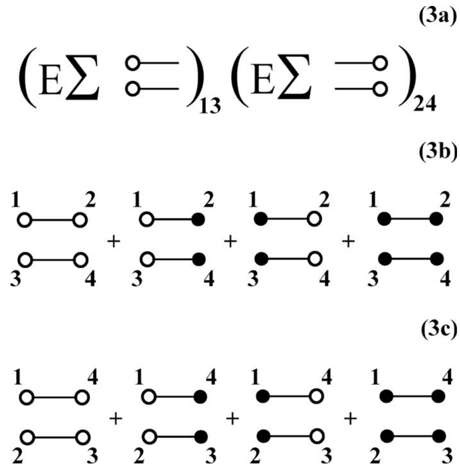

FIG. 3. The graphic depiction of the four-qubit Smolin states in Example 1.

$$\prod_{j=1}^{n}Z_j^{\gamma_j}|\mathrm{G}_n\rangle\langle\mathrm{G}_n|\prod_{j=1}^{n}Z_j^{\gamma_j}=\prod_{j=1}^{n}\left(\frac{\mathbf{1}+(-1)^{\gamma_j}g_j}{2}\right). \tag{17}$$

The associated colored graph of the $\Pi_{j=1}^{n}Z_j^{\gamma_j}|\mathrm{G}_n\rangle$ is G_n with colored vertices. The coloring rule is as follows. The j-th vertex is filled if the corresponding γ_j is 1 and blank if γ_j is 0. In addition, $\{\Pi_{j=1}^{n}Z_j^{\gamma_j}|\mathrm{G}_n\rangle | \forall \quad \gamma_j\in\{0,1\}\}$ forms a complete orthonormal set.

Moreover, in the following, edges can be divided into segments. The end of a segment is called unconnected if no vertex is attached. That is, a segment must have an unconnected end and attach a vertex. Two segments can be recovered into an edge. After the recovery, there is no unconnected end. As an illustration, we graphically describe the two-qubit state $Z_1|\mathrm{G}_2\rangle$ in equivalent twofold ways, which are shown in Fig. 1. The generic representation is shown in Fig. 1(a). In Fig. 1(b), two vertices each attach one divided edge.

Now, we consider the graphic depiction of the density matrix in Example 1, which is represented as Fig. 3. Therein, the notation $(\mathbf{E}\Sigma\ldots)$ denotes enumeration of the colored graph configurations with *even* filled vertices in the parentheses. For example, Fig. 2 illustrates the two-vertex case (without qubit index). To recover the edges, two segments in different parentheses are picked up and then these two unconnected ends are joined. For illustration purposes, Fig. 3(a) is to depict ρ_2 graphically, where the edges are divided and decomposed as the product form (the subscript is the vertex or, equivalently, qubit index). Different recovering ways indicate the different physical preparations. For instance, in Example 1, the vertex pairs (1, 2) and (3, 4) are graphically connected, as shown in Fig. 3(b), with the corresponding stabilizer generators are listed in Eq. (12). Notably, according to the constraints in Eqs. (10) and (11), both vertices 1 and 3 (2 and 4) are both either filled or blank. As for the corresponding preparation, two two-qubit connected graph states $|\mathrm{G}_2\rangle_{12}|\mathrm{G}_2\rangle_{34}$ are initially prepared. Then it is followed by the local operations $(X_1^iZ_1^j)$ and $(X_3^iZ_3^j)$, where the value of random variables i and j can be either 0 or 1. Similarly, if the stabilizer generators are listed in Eq. (13). Notably, according the constraints in Eqs. (10) and (11), both vertices 1 and 2 (3 and 4) are both either filled or blank. The corresponding mixed state can be graphically depicted as Fig. 3(c).

Before further proceedings, some remarks on the edge-recovering are made as follows. First, after the recovering, the summation of graph configurations is obtained. Two vertices i and j are always either connected or unconnected in each graph configuration. Second, there exists no unconnected end after the recovery process. In Example 3, it will be shown that such condition implicitly constraints the possible ways of edge-recovering.

B. Family of n^2-qubit USBESs and its relation with Greco-Latin squares

As a generalization of Smolin state in Example 1, we consider a specific class of n^2-qubit USBESs in the graph-state formalism ($n>2$). According to Sec. II, the parameters in Eq. (7) $m, n_1, \ldots, n_m$ are set equal to n. For our convenience, the qubits and the corresponding vertices are reindexed as i_j, where $1 \le i \le n$ and $1 \le j \le n$. All x_{i_j} in Eq. (4) are set equal to 1, $\forall\ i, j$. According to Eq. (6), the i-th qubit set $T_i = \{i_j | 1 \le j \le n\}$ can be recognized as comprising the n-qubit colored graph-state $\prod_{j=1}^{n} Z_{i_j}^{\gamma_{i_j}} |\mathrm{G}_n\rangle$. Therein, the operator g_{i_j} corresponds to stabilizer generators g_{i_j} of $|\mathrm{G}_n\rangle$, where

$$\mathrm{g}_{i_j} = X_{i_j} \prod_{i_k \in N(i_j)} Z_{i_k}, \ \forall\ j = 1, \ldots, n. \tag{18}$$

As a result, it is obvious that two qubits $i_j \in T_i$ and $i'_{j'} \in T_{i'}$ are separable if $i \neq i'$. the condition (a) is automatically satisfied.

Moreover, a specific n-vertex graph $\mathrm{G}_n = (\mathrm{V}, \mathrm{E})$ is exploited as the "*template*." After the edge-recovering, all associate graphs of the density matrix are the template graphs with different vertex index and coloring. For instance, in the Example 1, the two-vertex connected graph is the template graph. In the following, the associate graph G_n with colored vertices comprises vertices $1, 2, \ldots, n$. The density matrix of the n^2-qubit USBES is denoted by ρ_n. As a result, the j-th stabilizer generator g_j of ρ_n is

$$g_j = \prod_{i=1}^{n} \mathrm{g}_{i_j}, j = 1, \ldots, n. \tag{19}$$

Therefore, in the graphic representation, even number of the vertices in the corresponding qubit set $\{i_j | 1 \le i \le n\}$ must be filled. As for the graphical decomposition of ρ_n, the i_j-th vertices attaching the divided edges with the same index j are put in the j-th parentheses. To construct a colored-vertex graph (a) $\forall\ j$, pick a vertex i'_j from the unpicked vertices in the j-th parentheses. The i'_j-th vertex is exploited as the j-th vertex of the template graph. (b) According to the connections of the template graph, join the unconnected ends of the divided edges to construct G_n. (c) Repeat (a) and (b) until all the vertices in the parentheses are used up.

Interestingly, the Greco-Latin squares of order n can help the recovery of the edges. A Greco-Latin square or orthogonal Latin square of order n is an $n \times n$ arrangement of cells, such that (i) each cell containing an ordered pair (i,j), where $i, j \in \{1, 2, \ldots, n\}$, where every row and every column contains exactly one i and exactly one j, and (ii) no two cells contain the same ordered pair of symbols.

To recover the edges, the ordered pair (i,j) denote the vertex i_j. According the Greco-Latin square, the corresponding vertices in the same row (or column) are exploited to construct the template graph. In other words, the corresponding qubits can be regarded as comprising the corresponding colored graph state. The partitions Q_i and T_i are the sets of corresponding qubits in the i-th row. Two qubits are separable if their qubit indexes appear different rows in a Greco-Latin square.

Example 2. In Ref. [12], a nine-qubit system is considered as follows. Let

$$g_1 = \prod_{i=1}^{3} X_{i_1} Z_{i_2} Z_{i_3} \tag{20}$$

$$g_2 = \prod_{i=1}^{3} Z_{i_1} X_{i_2} Z_{i_3} \tag{21}$$

$$g_3 = \prod_{i=1}^{3} Z_{i_1} Z_{i_2} X_{i_3}. \tag{22}$$

The fully connected three-vertex graph is exploited as the template. For instance, a Latin squares of order 3 is

$$\begin{matrix} 11 & 22 & 33 \\ 23 & 31 & 12\,. \\ 32 & 13 & 21 \end{matrix} \tag{23}$$

For example, the ordered pair in the cell in first column and the first row indicates the vertex 1_1. According to the first, second, and the third rows of orthogonal Latin square in Eq. (23), the nine qubits are divided into three groups $T_1 = Q_1 = (1_1, 2_2, 3_3)$, $T_2 = Q_2 = (1_2, 2_3, 3_1)$, and $T_3 = Q_3 = (1_3, 2_1, 3_2)$, respectively. Vertices in the same group are exploited to construct the template graph. In such partition, qubits in the same group are separable from the qubits of the other groups.

Now we propose how to activate the entanglement of the USBESs in the following scenario. Suppose there are $2n-1$ distant parties. Wherein, $j \in \{1, 2, \ldots, (n-1)\}$, the j-th party holds the n qubits that correspond to the vertices in the j-th row of a Latin square of order n. The remaining n parties each hold a qubit that corresponds to one vertex in the n-th row. The goal is to activate the entanglement of the n qubits held by parties n, $(n+1)$, ..., and $(2n-1)$. To achieve this, the parties holding n qubits each perform the n-qubit projective joint measurement using the orthonormal basis $\{\prod_{i=1}^{n} Z_{i_j}^{\alpha_{i_j}} |\mathrm{G}_n\rangle \,|\, \alpha_{i_j} \in \{0,1\}\}$. Without loss of generality, let these $(n-1)$ post-measurement states are $\prod_{i=1}^{n} Z_{i_1}^{m_{i_1}} |\mathrm{G}_n\rangle$,

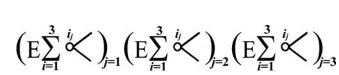

FIG. 4. The graphic decomposition of the nine-qubit USBES in Example 2. Notice that, in Figs. 4 and 5, the subscript j is not the exact vertex index.

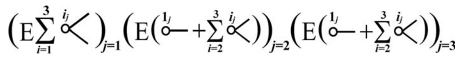

FIG. 5. The graphic decomposition of the nine-qubit USBES in Example 3.

$\Pi_{i=1}^{n} Z_{i_2}^{m_{i_2}}|G_n\rangle$, …, and $\Pi_{i=1}^{n} Z_{i_{(n1)}}^{m_{i_{(n-1)}}}|G_n\rangle$, respectively. The unmeasured n-qubit entangled state now becomes $\Pi_{i=1}^{n} Z_{i_n}^{m_{i_n}}|G_n\rangle$. Wherein, since $\Pi_{i=1}^{n} g_{i_j}$ is the stabilizer generator, we have

$$\sum_{i=1}^{n} m_{i_j} = 0 \bmod 2 \ \forall \quad j \in \{1, \ldots, n\}. \tag{24}$$

Consequently, at last, the j-th party ($j \neq n$) publics the binary message vectors $(m_{1_j}, \ldots, m_{n_j})$. The values of $m_{1_n}, \ldots, m_{n_n}$ can be induced using Eq. (24). Therefore, the entanglement can be activated.

IV. DISCUSSIONS

Note that there is high permutation symmetry in the USBESs in the previous section. In the following example, the USBES with lower symmetry is considered.

Example 3. Here, we consider the nine-qubit USBES. Therein, stabilizer generators g_1 is the same as that in Eq. (20), and g_2 and g_3 now are modified as

$$g_2 = Z_{1_1} X_{1_2} I_{1_3} \prod_{i=2}^{3} Z_{i_1} X_{i_2} Z_{i_3} \tag{25}$$

$$g_3 = Z_{1_1} I_{1_2} X_{1_3} \prod_{i=2}^{3} Z_{i_1} Z_{i_2} X_{i_3}. \tag{26}$$

The graphics decomposition is shown in Fig. 5. Wherein, Latin square cannot help design the edge-merging. Moreover, the vertices 1_2 and 1_3 both must be connected with the same vertex $i_1, i \in \{1,2,3\}$, to comprise the three-vertex linear graph.

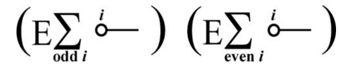

FIG. 6. The graphic depiction of the $2m$-qubit USBES in Example 4.

As the end of the paper, we consider $2m$-qubit USBES [11].

Example 4. Two stabilizer generators of $2m$-qubit USBES are

$$g_1 = \prod_{i=1}^{m} X_{2i-1} Z_{2i} \tag{27}$$

$$g_2 = \prod_{i=1}^{m} Z_{2i-1} X_{2i}. \tag{28}$$

Such USBES is locally equivalent to the one proposed by Bandyopadhyay and co-workers [7,11,12]. The density matrix can be graphically depicted in Fig. 6.

In conclusion, we investigate multipartite unlockable stabilized bound entanglement in both algebraic and graphic ways. Algebraically, the substantial mathematical structure is studied. On the basis of graph states, it is also found that such bound entangled state can be graphically depicted, which can be represented in the decomposition form.

ACKNOWLEDGMENTS

The authors acknowledge financial support from the National Science Council of the Republic of China under Contract No. NSC.96-2112-M-033-007-MY3. This work is partially supported by the Physics Division of the National Center of Theoretical Sciences.

[1] C. H. Bennett, G. Brassard, C. Crepeau, R. Jozsa, A. Peres, and W. K. Wootters, Phys. Rev. Lett. **70**, 1895 (1993).
[2] C. H. Bennett and S. J. Wiesner, Phys. Rev. Lett. **69**, 2881 (1992).
[3] A. K. Ekert, Phys. Rev. Lett. **67**, 661 (1991).
[4] C. H. Bennett, H. J. Bernstein, S. Popescu, and B. Schumacher, Phys. Rev. A **53**, 2046 (1996).
[5] M. Horodecki, P. Horodecki, and R. Horodecki, Phys. Rev. Lett. **80**, 5239 (1998).
[6] J. A. Smolin, Phys. Rev. A **63**, 032306 (2001).
[7] R. Augusiak and P. Horodecki, Phys. Rev. A **73**, 012318 (2006).
[8] L.-Y. Hsu, Phys. Rev. A **76**, 032311 (2007).
[9] R. Augusiak and P. Horodecki, Phys. Rev. A **74**, 010305(R) (2006).
[10] W. Dür, J. I. Cirac, and P. Horodecki, Phys. Rev. Lett. **93**, 020503 (2004).
[11] S. Bandyopadhyay, I. Chattopadhyay, V. Roychowdhury, and D. Sarkar, Phys. Rev. A **71**, 062317 (2005).
[12] G. Wang and M. Ying, Phys. Rev. A **75**, 052332 (2007).
[13] J. Preskill, *Lecture Notes for Physics 229: Quantum Information and Computation* (Cambridge University Press, Cambridge, England, 1998).